

Wigner quasi-particle attributes—An asymptotic perspective

M. Nedjalkov,¹ P. Schwaha,^{1,a)} S. Selberherr,¹ J. M. Sellier,² and D. Vasileska³

¹*Institute for Microelectronics, TU-Wien, Vienna 1040, Austria*

²*IICT, Bulgarian Academy of Sciences, Sofia 1113, Bulgaria*

³*School of Electrical, Computer, and Energy Engineering, Arizona State University, Tempe, Arizona 85287-5706, USA*

(Received 23 December 2012; accepted 11 April 2013; published online 24 April 2013)

Wigner quantum mechanics is reformulated in a discrete momentum space and analyzed within a Monte Carlo approach for solving integral equations and thus associated with a particle picture. General quantum phenomena may thereby be modeled in terms of quasi-particles involving attributes such as drift, generation, sign, and annihilation on a phase space grid. The model is examined in an ultimate regime, where classical and quantum dynamics become equivalent. The peculiarities of the transport in this asymptotic regime are analyzed within simulations, benchmarking the behavior of the Wigner function. © 2013 AIP Publishing LLC. [<http://dx.doi.org/10.1063/1.4802931>]

Classical physical quantities are presented by phase space dynamical functions A_p , having equations of motion determined by the Poisson bracket. Operator mechanics associates operators \hat{A} which evolve according to the commutator with the Hamiltonian. The difference between the mean values of A_p and \hat{A} may be evaluated by an inference,¹ estimating how long classical and quantum evolutions stay close, within a prescribed error. The manner in which the commutator tends towards the Poisson bracket is explored in the classical limit $\hbar \rightarrow 0$. This, in quantum theories, widely applied formal limit refers to the behavior of certain physical quantities, attached to \hbar —in this case, these are energy and time.

These considerations become more intuitive in the Wigner formulation of quantum mechanics, where states and physical observables are defined in the phase space once more. Classical evolution is determined by the first derivative of the electric potential—the electric field, accounted for by the Liouville part of the Boltzmann equation. In contrast, quantum evolution is governed by the entire potential, which is used to define the Wigner integral operator. The Taylor expansion of the latter couples the derivatives of the potential with the powers of \hbar . This represents another form of the limit $\hbar \rightarrow 0$, which is survived only by the electric field. In this case, the Wigner equation reduces to the ballistic Boltzmann counterpart and the difference between classical and quantum pictures is imposed by the initial state. In this treatment, we consider coherent problems, effects from scattering and statistical aspects will be regarded elsewhere. The physical states are subsets of the much broader class of solutions allowed by any of these equations. Then, a legitimate quantum state must obey a condition related to the uncertainty relation,^{2,3} while the classical state must be non-negative, and is actually interpreted as initial distribution of point like particles. This duality offers a transparent classical process, which may be used as a reference for validation of quantum transport simulation methods. However, this approach has not yet been applied in the case of Wigner transport, because the involved generalized functions

preclude any direct numerical treatment. This research aims both to develop an asymptotic approach to the problem and to validate a Wigner particle model under such extreme conditions.

Wigner models of carrier transport phenomena conveniently utilize basic similarities between classical and quantum notions in phase space. Alternative concepts such as Wigner trajectories,⁴ quantum windows in Monte Carlo (MC) regions,⁵ consecutive coupling of Boltzmann, and Wigner regions⁶ have been explored. However, a well established approach is still missing, as any of the developed models meets certain numerical challenges. Deterministic methods^{7,8} exhibit problems with discretization⁹ and can treat only single-dimensional transport, because the efforts for matrix inversion become enormous. The development of stochastic approaches began during the last decade, when the phenomenological Monte Carlo approach, hindered by the existence of negative values in the quantum quasi-distribution, was replaced by more formal methods. Two particle models have been derived, currently unified by the trend to reuse major parts of the classical transport concepts. Ensemble MC particles endowed with affinity—an attribute carrying the value of the quantum potential—have been shown to be an adequate approach to single-dimensional carrier dynamics.⁹ A multi-dimensional application is hindered by the enormous computational requirements posed by the increase of the number of needed particle states in the ensemble. The second model is a single particle MC approach, based on the ergodicity of the system and thus restricted to stationary transport determined by the boundary conditions.¹⁰ When compared to the affinity approach, it has very different attributes, related to generation of signed particles. These reside on phase space points of generation, waiting to be consecutively evolved to the boundary. If an evolving particle meets a resident counterpart with opposite sign, both particles annihilate each other—a property which spares the efforts to evolve them to the boundary. As the probability for a trajectory to meet at a point is zero, this property is approximated using a cell in a phase space grid. The last object introduced is that of a momentum subspace grid, which appears to be inherent to the stationary Wigner function.¹¹ Despite this variety of concepts and attributes, there is no

^{a)}Present address: AVL List GmbH, Hans-List-Platz 1, 8020 Graz, Austria.

universal model; thus, the main challenge is to identify and utilize the ones, which may be unified in a particle model relevant for general transport conditions while maintaining moderate computational demands.

We exploit the concepts of momentum quantization, indistinguishable particles and renormalization by annihilation at consecutive time steps. Entangled with the notions of classical trajectories, particle ensemble, particle generation, and sign give rise to a time-dependent fully quantum transport model which naturally includes both open and closed boundary conditions along with general initial conditions. The model is introduced in the next section by a reconsideration of the usual continuous formulation of Wigner dynamics. It is then applied in an asymptotic approach to quantum-classical evolution duality.

In contrast to the transport problem formulated in terms of a density matrix $\rho(r+s, r-s)$, the Wigner counterpart may be easily formulated in a confined domain of r .¹² The definition involves the integral Fourier transform $FD\{\}$ of ρ over s . We maintain that a discrete transform conforms better with the principles of quantum mechanics applied to nano structures. Indeed, ρ is zero always when s is outside the physical boundaries, while in the contacts the correlation “heals”⁸ over several thermal momentum lengths, or even already when entering the contact.¹³ Thus, a minimal characteristic length L may be specified for the unitary transform giving the Wigner function $f(r, n, t)$ in terms of a discrete momentum:

$$f(n, \cdot) = \frac{1}{L} \int_{-L/2}^{L/2} ds e^{-i2n\Delta ks} \rho(s, \cdot) = FD\{\rho(s, \cdot)\}, \quad (1)$$

$$\rho(s, \cdot) = \sum_{n=-\infty}^{\infty} e^{i2n\Delta ks} f(n, \cdot); \quad \Delta k = \pi/L. \quad (2)$$

Traditionally, the numerical aspects are presented in terms of Δk , but this is a convenient shortcut of $\Delta p/\hbar$ —relevant for the physical analysis is the momentum p . The Wigner equation

$$\left(\frac{\partial}{\partial t} + \frac{\hbar n \Delta k}{m} \frac{\partial}{\partial r} \right) f(r, n, t) = \sum_{n'} V_w(r, n - n') f(r, n', t), \quad (3)$$

$$V_w(r, n) = \frac{1}{i\hbar} FD\{(V(r+s) - V(r-s))\} \quad (4)$$

involves the sum over the Wigner potential $V_w(n, r)$, which now may depend on the time.

Equation (3) is first reformulated as a Fredholm integral equation of the second kind. The time integral is introduced by field less Newton’s trajectories linking the solution $f(r, n, t)$ back in time to the two components of the free term f_0 containing the initial and the boundary conditions. Then, a proper adjointed equation is derived, which allows to express the expectation value as a series

$$\langle A \rangle_t = \langle f_0 A \rangle_t + \langle f_0 \Gamma A \rangle_t + \langle f_0 \Gamma \Gamma A \rangle_t + \dots \quad (5)$$

of a generic physical quantity A , e.g., velocity or energy. The consecutive terms in the brackets are linked by expressions

having a meaning of free flight over forwardly—in time—parametrized trajectories. Γ is given by three terms having a meaning of scattering sources

$$\Gamma(r, m, m') = V_w^+(r, m - m') - V_w^-(r, m' - m) + \gamma(r) \delta_{m, m'} \quad (6)$$

with

$$V_w^+ = \begin{cases} V_w & \text{if } V_w > 0 \\ 0 & \text{otherwise} \end{cases} \quad \gamma(r) = \sum_{m=-\infty}^{\infty} V_w^+(r, m)$$

and $V_w^-(m) = V_w^+(-m)$. The terms in Eq. (6) have equal total rate γ , which allows for the following interpretation: after any free flight, the trajectory forks into three: the initial trajectory continues due to the Kronecker delta, and two trajectories are initiated with offset of $l = m - m'$ and of $-l$ around the initial momentum number.

A particle picture can be associated with the expansion (5). Particles, distributed and initialized by a sign according to the initial and boundary condition values, begin free flights over Newton trajectories. With a frequency determined by γ , these particles create couples of particles at random times $t' < t$ locally in r and with offset $\pm l$ in momentum number space until reaching the evolution time t . The particle in l carries the sign of the parent particle, the counterpart bears the opposite sign. These child particles generate further couples which also evolve until time t . Those which leave the boundaries are neglected, the remaining contribute to the value of Eq. (5) according to their sign. In this sense, contributions from particles having the same momentum number and position, but with opposite signs compensate each other: particle annihilation still occurs but at the end of the evolution, at the recording of the particles states. Due to the Markovian character of the latter, the ensemble state may be evolved at consecutive time steps, where the final state obtained by recording on a phase space grid becomes the initial condition for the next step in the evolution. The model has passed the standard comparison with other quantum approaches, which will be reported elsewhere.

We summarize some of the peculiarities of this method: The momentum subspace becomes discrete, so that exact generation-annihilation rules are specified. The standard ensemble of enumerable particle states containing the particular position and momentum coordinates and time is replaced by an array of signed integers associated with phase space nodes. These integers on a grid comprise the concept for indistinguishable particles (we note the difference with the common statistical meaning of the phrase, where it usually indicates certain symmetry of the physical state), whose number may grow without causing any memory problems.

Numerical discretization is needed only for the position variable r , where the Wigner function is smooth, as is guaranteed by the existence of the gradient in Eq. (3).

The simulations presented in the next section explore the compatibility of these particle attributes in the discussed asymptotic regime.

The equivalence between ballistic Boltzmann and Wigner evolution is established for linear potentials Ex by the following equality:

$$\int dk' V_w(\cdot, k - k') f(\cdot, k') = -\frac{eE\partial f(\cdot, k)}{\hbar\partial k}. \quad (7)$$

Quantum effects may be introduced only by the initial condition and thus are discarded by the choice $f_0 = N\delta(k)\delta(x)$. The latter indicates the involved physics as all other initial functions are superpositions of f_0 . According to the Boltzmann counterpart, the evolution corresponds to an acceleration of N classical particles, over a common Newton trajectory. The challenge now is to model the process within the signed particle scheme. The electric force is incorporated via the electric field in the Wigner potential so that no direct acceleration is possible in this picture. The effect of acceleration may be achieved only by the generation of positive and negative particles. Unfortunately, the equality (7) reveals the Wigner potential as a delta function derivative δ' . The equality relies on the integral Fourier transform, which is formally obtained by the limit $L \rightarrow \infty$ of the discrete counterpart ($1/L$ becomes $1/2\pi$) corresponding to the continuous formulation of Eqs. (1)–(4). In this case, the classical limit ensured by the diverging coherence length is another manifestation of the formal limit $\hbar \rightarrow 0$ giving rise to continuous momenta: $\Delta p = \pi/(L/\hbar) \rightarrow 0$. The mathematical aspects of the convergence towards the continuous solution and the role of \hbar are explored in Ref. 14. The existence of generalized functions precludes any exact numerical treatment. In particular, the definition of the Wigner potential (4) diverges for a linear potential in this limit.

A relevant numerical approach relies on a finite L , so that the Wigner potential is

$$V_w(x, n) = -\frac{eEL \cos(\pi n)}{\hbar\pi} \frac{1}{n}. \quad (8)$$

We analyze the impact this assumption has on any of the two transport regimes. The Boltzmann description is influenced by the discretization $\Delta k = \pi/L$, which imposes cellular automata evolution rules¹⁵ for the accelerated particles: The probability for a transition during a time dt between the initial and the next node in field direction is proportional to the acceleration $dk = eEdt/\hbar$. The particle number N gradually decreases with time at the initial node, while the number on the next node increases accordingly. For a time Δt given by the Newton law: $\Delta k = eE\Delta t/\hbar$, all particles are transferred to the next node, which corresponds to the same momentum value, which would be obtained if they were continuously accelerated by the field.

The same process is observed when applying the quantum method: in Fig. 1, the initial density at $k=0$ gradually decreases, while the density on the first node to the right increases. The initial peak drops, so that for 0.52 ps their number on the adjacent nodes becomes equal. Then, for around 1 ps the initial $N = 10^5$ particles appear on the first node: for $E = 10^4$ V/m and $L = 200$ nm this time is consistent with Newton's law: $\Delta k = eE\Delta t/\hbar$. Particles gain momentum with a time which corresponds to acceleration; however, the latter is obtained not by the classical particle transfer, but within the sign generation-annihilation model. Theoretical considerations show that, according to Eq. (8) only positive particles are generated at the first node, while only negative

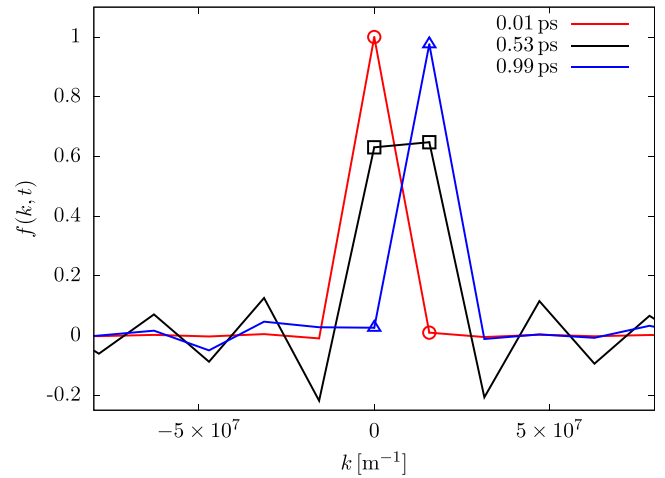


FIG. 1. Evolution of the normalized density $f(k, t)$. The initial, intermediate, and final particle densities in the two adjacent peaks are outlined around the origin by symbols. The acceleration of the initial peak is accompanied with unphysical effects of density oscillations away from the origin.

particles are generated at the origin thus decreasing the initial peak.

However, there is more than this desired behavior of the evolution process. We observe a persistent pattern of positive and negative densities, which covers the whole domain, and is present in all of the figures. This behavior is the price paid for the step back from the initially continuous picture: equivalence between Wigner and Boltzmann transport is guaranteed only when $L \rightarrow \infty$. The discrete case follows quantum rules, so that the whole system is disturbed by the violation of the uncertainty principle in the initial condition. The oscillations initially resemble the pattern of Eq. (8) and near to the origin increase with the evolution time above 20% of the initial peak. When the number of particles on the first node begins to dominate, the inverse process of decrease begins. At the end, when all particles are at the first node, the oscillations are significantly damped, Fig. 1. The pulsing of the non-classical component of the solution can be explained by theoretical considerations: particles generated from the first node according to Eq. (8) are of inverse polarity when compared to those generated from the initial node. It is related to the offset Δk corresponding to a switch from n to $n + 1$ in Eq. (8) and thus a flipping of the sign. Thus, in a distant node X , we first observe accumulation of particles with a certain sign due to the initial condition, which is further compensated by the particles appearing due to the first node, which at the distant node X , generate particles of opposite sign. The density is closest to the classical shape at discrete points in time, showing that the classical picture is approximated at consecutive steps Δt , which tend to zero with Δk . Accordingly, the decrease of the latter causes a decrease of the magnitude of the oscillations as confirmed numerically in Fig. 2. However, this unphysical solution provides a fine structure to explore the effect of annihilation on the precision of the model. Fig. 3 shows a snapshot of the distribution at 0.9 ps obtained for three different steps for recording. The results are in excellent agreement, reference is the 1×0.9 ps curve corresponding to the highest precision for Eq. (5), which demonstrates the reliability of the method. Furthermore, the annihilation greatly improves the computations as the particle number increases

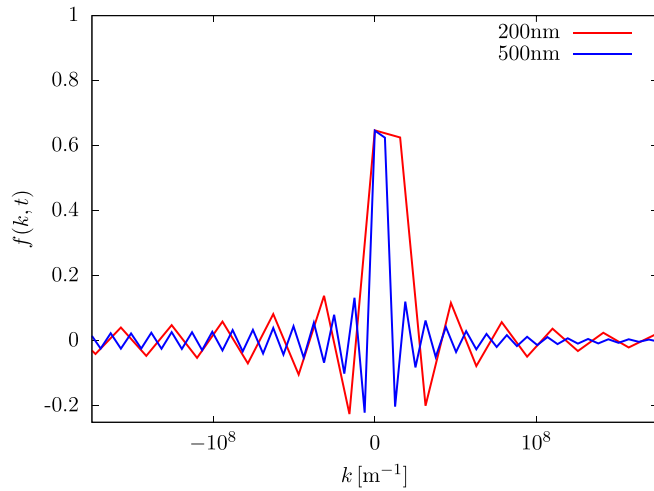


FIG. 2. With the increase of the coherence length L from 200 nm to 500 nm, the magnitude of the non-classical component of the solution decreases along with the shortening of the oscillating period according to $\Delta k = \pi/L$. The evolution time is 0.5 ps.

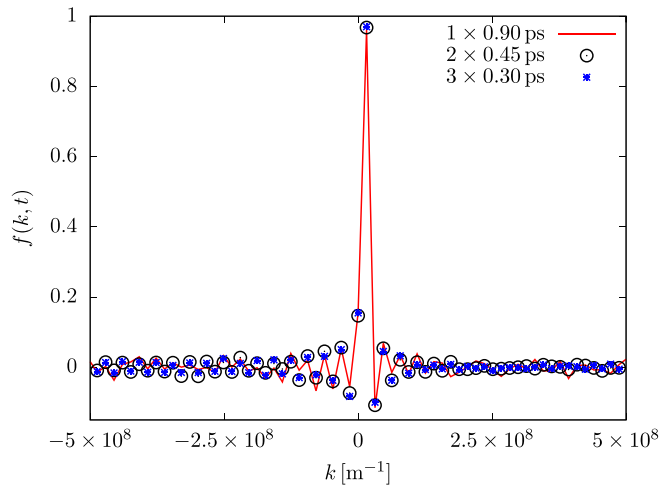


FIG. 3. The fine structure of the density is used to explore the effect of annihilation. The results from a direct simulation of the 0.9 ps evolution, a single intermediate recording, the 2×0.45 ps curve, and two intermediate recordings, the 3×0.3 ps curve, are in excellent agreement.

exponentially with the evolution time: the 3×0.3 ps simulation involves three orders of magnitude less particles compared to the reference simulation.

Finally, the method is capable to cleanly reproduce the acceleration of the initial condition for 5 ps evolution, Fig. 4, which is above the characteristic times of most transport processes in nano structures.

The announced general purpose ensemble carrier transport model overcomes the typical computational requirements for quantum simulations due to the concepts for indistinguishable particles and annihilation. The model may be regarded as a step towards unification between affinity and sign approaches and has potential for extension above

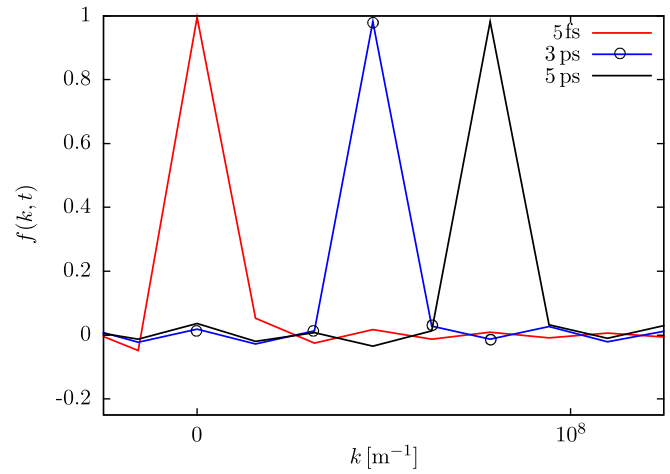


FIG. 4. The method maintains a clean picture of acceleration for 5 ps keeping the initial distribution intact. The position K of the peak at this time is consistent with the position which would be reached by Boltzmann particles accelerated according to the Newton law: $K = 5 \text{ ps} \times eE/\hbar$.

single-dimensional transport. The model is both validated and used to explore the transport regime asymptotically approaching the quantum-classical evolution duality. The underlying physics is a rich combination of classical and quantum effects. The latter disappear in a limit, which is an alternative manifestation of the fundamental bound $\hbar \rightarrow 0$. The fine structure of the asymptotic solution makes it a good candidate for benchmarking quantum transport models in phase space.

This work has been supported by the Austrian Science Fund (FWF) Project P21685-N22, the EC FP7 Project AComIn (FP7-REGPOT-2012-2013-1), and the Bulgarian NSF Grant DMU 03/61.

- ¹M. Nedjalkov, S. Selberherr, D. K. Ferry, D. Vasileska, P. Dollfus, D. Querlioz, I. Dimov, and P. Schwaha, *Ann. Phys.* **328**, 220–237 (2013).
- ²V. I. Tatarskii, *Sov. Phys. Usp.* **26**, 311–327 (1983).
- ³N. C. Dias and J. N. Prata, *Ann. Phys.* **313**, 110–146 (2004).
- ⁴K. L. Jensen and F. A. Buot, *Appl. Phys. Lett.* **55**, 669–671 (1989) and the references therein.
- ⁵J. Garcia-Garcia, F. Martin, X. Oriols, and J. Sune, *Appl. Phys. Lett.* **73**, 3539–3541 (1998).
- ⁶J. Garcia-Garcia and F. Martin, *Appl. Phys. Lett.* **77**, 3412–3514 (2000).
- ⁷W. R. Frensley, *Rev. Mod. Phys.* **62**, 745–789 (1990).
- ⁸N. C. Klusdahl, A. M. Krizan, D. K. Ferry, and C. Ringhofer, *Phys. Rev. B* **39**, 7720–7734 (1989).
- ⁹D. Querlioz and P. Dollfus, *The Wigner Monte Carlo Method for Nanoelectronic Devices* (ISTE-Wiley, 2010).
- ¹⁰M. Nedjalkov, H. Kosina, S. Selberherr, C. Ringhofer, and D. K. Ferry, *Phys. Rev. B* **70**, 115319 (2004).
- ¹¹M. Nedjalkov and D. Vasileska, *J. Comput. Electron.* **7**, 222–225 (2008).
- ¹²F. Rossi, A. Di Carlo, and P. Lugli, *Phys. Rev. Lett.* **80**, 3348–3351 (1998).
- ¹³G. Ferrari, P. Bordone, and C. Jacoboni, *Phys. Lett. A* **356**, 371–375 (2006).
- ¹⁴T. Goudon, *SIAM J. Numer. Anal.* **40**, 2007–2025 (2002).
- ¹⁵G. Zandler, A. Di Carlo, K. Krometer, P. Lugli, P. Vogl, and E. Gornik, *IEEE Electron Device Lett.* **14**, 77–79 (1993).